Geology of Proterozoic outcrops in Dead Man and Little San Nicolas Canyons, southern San Andres Mountains, New Mexico

Pamela J. Roths, 1991, pp. 91-96

in:
Geology of the Sierra Blanca, Sacramento, and Capitan Ranges, New Mexico, Barker, J. M.; Kues, B. S.; Austin, G. S.; Lucas, S. G.; [eds.], New Mexico Geological Society 42nd Annual Fall Field Conference Guidebook, 361 p.

This page is intentionally left blank to maintain order of facing pages.

GEOLOGY OF PROTEROZOIC OUTCROPS IN DEAD MAN AND LITTLE SAN NICOLAS CANYONS, SOUTHERN SAN ANDRES MOUNTAINS, NEW MEXICO

PAMELA ROTHS
Programs in Geosciences, University of Texas at Dallas, Richardson, Texas 75080

Abstract—Proterozoic outcrops in the southern San Andres Mountains generally consist of large granitic plutons. However, isolated areas, such as Dead Man and Little San Nicolas Canyons, contain other rock types. A sequence of interbedded schists and fine-grained quartzites overlain by a crossbedded, micaceous quartzite is exposed in Dead Man Canyon. Three generations of folding have been identified: (1) early isoclinal folds perhaps synchronous with the metamorphism; (2) open to tight folds with a well-developed axial planar cleavage that strikes northwest; and (3) east-trending reclined folds that reorient the earlier structures into broad kinks. A foliated pluton dated at 1632 ± 24 Ma (U-Pb zircon) defines a maximum age for the second phase of deformation. Little San Nicolas Canyon, approximately 32 km south of Dead Man Canyon, contains high-grade gneiss, amphibolite and non-foliated granitic rock. The gneiss displays a foliation, defined by bands of dark and light minerals, that has been folded into tight to isoclinal east-trending folds. This unit is exposed along high-angle reverse faults. Zircons from the gneiss are highly discordant, but yield an age of 1730 ± 130 Ma. The protolith of this gneiss is unknown, but is most likely plutonic. One post-orogenic granite has been dated at 1460 ± 65 Ma. Although both study areas display similar east-west structural trends, they are markedly dissimilar.

INTRODUCTION

The San Andres Mountains contain a 140-km-long exposure of Proterozoic rock (Fig. 1). These outcrops are exposed along the eastern side of the range, where they are unconformably overlain by more than a thousand meters of mostly marine Paleozoic and Cretaceous strata. According to Seager (1981), several periods of faulting have affected this area. In Laramide time (40 to 60 Ma), steeply dipping thrust faults formed along the eastern flank of the range. Block faulting began in late Tertiary time, tilting the strata to the west and exposing the Precambrian core. More recently, widely spaced range-boundary faults with associated horsts and grabens have developed. Motion along the eastern range-boundary fault of the San Andres Mountains has persisted to within the last 4000 to 5000 yrs (Seager, 1981).

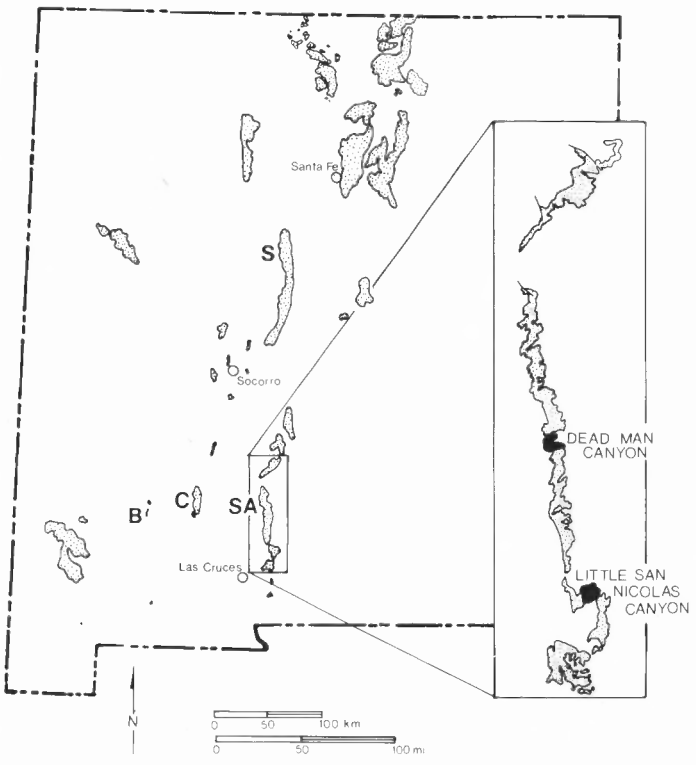

FIGURE 1. Location map showing Precambrian outcrops in New Mexico. S, Sandia Mountains; B, Black Range; C, Caballo Mountains; SA, San Andres Mountains. Inset shows location of study areas (shaded) in southern San Andres Mountains.

The Proterozoic rocks of southern New Mexico have received little attention, owing to the small, scattered outcrops. Previous work in southern New Mexico includes Condie and Budding (1979), Stacey and Hedlund (1983), Bauer and Lozinsky (1986) and White (1977).

This work was conducted as part of a regional study of the Proterozoic rocks of west Texas and southern New Mexico. The New Mexico portion of the project included mapping areas of the southern San Andres Mountains, determining a deformation history for these areas, and dating of select rock units by U-Pb zircon methods. Reconnaissance maps by Condie and Budding (1979) were used to choose the study areas. Although most of the Proterozoic units exposed in the San Andres Mountains are plutonic, there are several large exposures of older metamorphic rock. Two of these exposures are in Dead Man and Little San Nicolas Canyons (Fig. 1). The northern area, Dead Man Canyon, is covered by the Gardner Peak USGS 7.5-min quadrangle, and the southern area, Little San Nicolas Canyon, is located on the Bennett Mountain USGS 7.5-min quadrangle. Thirteen days were spent mapping and collecting samples in Dead Man Canyon; five in Little San Nicolas Canyon.

As they are located within White Sands Missile Range, access to the San Andres Mountains is restricted. Permission to enter the Range must be obtained 30 days in advance, and all visitors must be accompanied by range personnel. The Army will provide four-wheel-drive field vehicles.

DEAD MAN CANYON AREA

A simplified geologic map covering an area of 34 km^2 (13 mi^2) in Dead Man Canyon is shown in Fig. 2. The Proterozoic section comprises fine-grained schists and quartzites. Sedimentary structures are often well preserved. Interbedded fine-grained, highly siliceous units and several foliated biotite-bearing amphibolites are interpreted as metamorphosed felsic tuffs and basalt flows or sills. The foliated amphibolites are more common in the southern portion of the study area.

A medium- to coarse-grained, micaceous quartzite, with well-developed trough crossbedding, overlies the thin-bedded schists and fine-grained quartzites (shown as p€q on Fig. 2 and Fig. 3). The contact between this quartzite and the underlying schistose metasediments appears conformable.

Two plutons intrude the metasediments. The older pluton (p€g$_f$ on

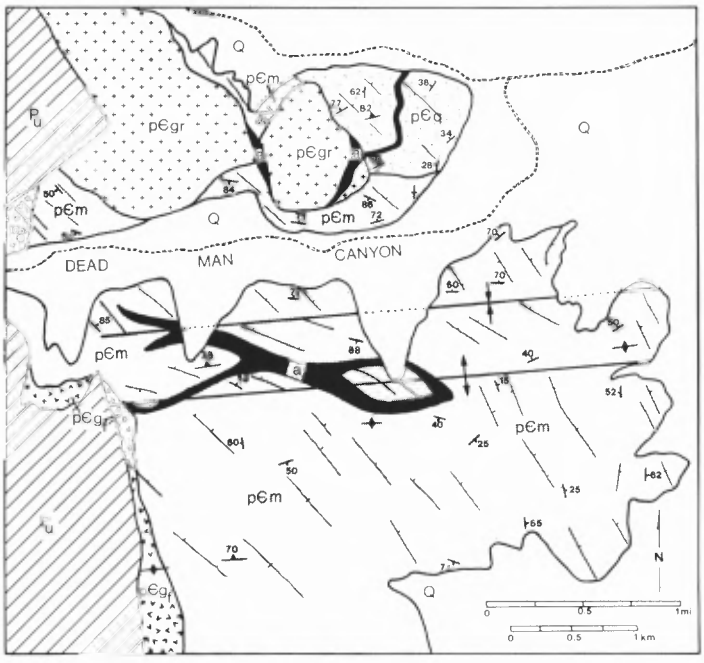

FIGURE 2. Simplified geologic map of the Dead Man Canyon area. pЄgr, unfoliated Mayberry pluton; pЄgf, foliated granite; pЄq, quartzite; pЄm, metasediments; a, Precambrian amphibolite; P_u, undifferentiated Paleozoic; Q, Quaternary alluvium. A sandstone bed in the quartzite is shown in black. Strike and dip symbols mark bedding and toothed lines mark crenulation cleavage (S_3) readings. Trace of S_3 axial planes shown. Fine lines mark trend of slaty cleavage (S_2) with tick marks showing direction of dip. Filled circle marks sample location. See Fig. 1 for location of Dead Man Canyon.

FIGURE 3. Crossbedded quartzite found in the northern end of the Dead Man Canyon study area. Note the steeply dipping cleavage (S_2) that crosscuts the bedding. Scale is 15 cm.

Fig. 2), a coarse-grained quartz monzonite, contains two foliations. The contact between this pluton and the country rock is highly discordant, with the metasedimentary units striking at high angles to the contact with the pluton. The younger pluton, the Mayberry pluton (pЄgr on Fig. 2; Condie and Budding, 1979), is an undeformed medium-grained quartz monzonite that intrudes the entire metasedimentary package.

A large unfoliated amphibolite body intrudes the metasedimentary succession along the south side of Dead Man Canyon and several large xenoliths of similar mafic rock occur in the Mayberry pluton. The contact of the amphibolite with the country rock is generally concordant. These unfoliated mafic rocks are composed primarily of amphibole and plagioclase, with subordinate quartz.

Structural analysis

The units exposed in Dead Man Canyon show evidence of three generations of folding: (1) early, isoclinal folds marked by a bedding-parallel schistosity (S_1); (2) tight to isoclinal folds with a well-developed slaty cleavage (S_2); and (3) open kink folds with an associated crenulation cleavage (S_3). The earliest generation of structures is defined by a penetrative schistosity that is only present in more pelitic members of the metasedimentary rocks. This schistosity is subparallel to lithologic contacts, and in some outcrops is associated with isoclinal, intrafolial folds. These folds generally have a wavelength of 3 to 8 cm, and an amplitude of about 5 cm. The quartzites, particularly the upper micaceous quartzite, show no evidence of this early schistosity or intrafolial folding that is characteristic of the schists. The lack of development of the earliest fold structures in the quartzites is most likely related to increased competence of the quartzite layers.

The second phase of deformation produced the dominant fabric found in the study area, a well-developed slaty cleavage (S_2) that folds both bedding (S_0) and the schistosity (S_1). The orientation of this cleavage is generally N50°W and it dips steeply to the northeast. In an area along the south side of Dead Man Canyon, the S_2 slaty cleavage is reoriented to N70°W. An example of both the N50°W-striking and the N70°W-striking folds is given below.

The best example of the folds that strike N50°W is found in the upper quartzite (pЄq on Fig. 2). This quartzite is folded into a syncline that strikes N50°W and plunges moderately to the west (Fig. 4a). The syncline has a rounded hinge and limbs and an interlimb angle of 90°. Axial planar cleavage is well developed (Fig. 3). The F_2 folds in the interbedded schists and quartzites below the micaceous quartzite have similar characteristics (Fig. 5).

Along the south side of Dead Man Canyon, the F_2 slaty cleavage strikes N70°W, dips steeply to the north, and is associated with a nearly isoclinal fold (Fig. 4b). This tighter fold occurs in a schistose portion of the sedimentary section, so the greater strain may be due to less competent rock types. Also, the axial plane is approximately parallel to the axial plane of the later crenulation cleavage (S_3), so this fold may have been modified to a greater extent during the final phase of deformation (F_3).

The distribution of poles to the slaty cleavage (S_2) described above and mesoscopic fold axes (L_2) indicate that they have been refolded around an axis that plunges steeply to the north-northwest during D_3 (Fig. 4c). The L_3 fold axis plunges 80° to N20°E, and the S_3 axial plane strikes N85°E and dips 80°N (Fig. 4d). The S_3 cleavage is weakly developed throughout the study area. F_3 folds are reclined, with sharp hinges and planar limbs. They are highly asymmetrical with interlimb angles of 160°.

Geochronology

Zircons were separated from suitable rock units and treated as described in the Appendix. The ages listed in this paper supercede those published in Roths (1991). Discordant zircons from the older, foliated pluton yielded a U-Pb isotopic age of 1632 ± 24 Ma (MSWD = 0.81; Fig. 6). This pluton contains both the earlier slaty cleavage and the E-W crenulation fabric, and so either predates both events or is syntectonic with respect to D_2. Therefore, the maximum age for D_2 is 1632 ± 24 Ma. The undeformed pluton, the Mayberry granite, lacks zircon, and was not suitable for U-Pb dating. White (1977) determined an age of 1248 ± 170 Ma, with an initial strontium ratio of .7463 for this pluton, using Rb-Sr whole-rock methods (recalculated using decay constants of Steiger and Jager, 1977).

Summary and discussion

The metasedimentary rocks exposed in Dead Man Canyon are composed of interbedded fine-grained quartzites and schists. At the top of the section is a trough crossbedded, micaceous quartzite. Three phases of folding have affected these rocks. The first phase resulted in bedding-parallel schistosity in the mica-rich units, associated with isoclinal,

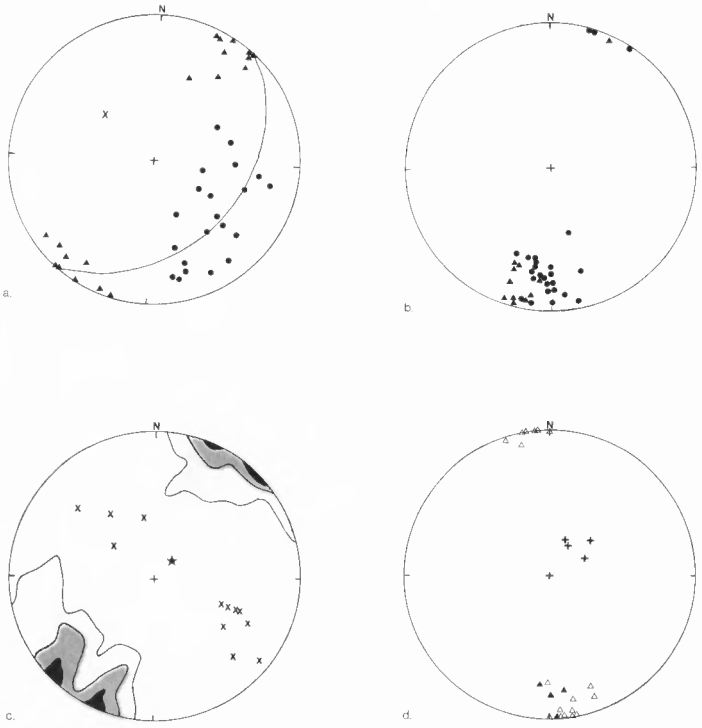

FIGURE 4. Lower hemisphere, equal-area stereonets of bedding and cleavage data from Dead Man Canyon. a, Poles to bedding and cleavage from syncline exposed in the quartzite north of Dead Man Canyon. Filled circles are poles to bedding; triangles, poles to cleavage; X, pole to best-fit great circle. b, Poles to bedding and slaty cleavage from area south of Dead Man Canyon. Filled circles are poles to bedding; triangles, poles to slaty cleavage. c, Poles to 235 slaty cleavage (S_2) measurements in Dead Man Canyon area. Contour intervals are 2, 10, and 20%. X, mesoscopic fold axes associated with slaty cleavage (S_2); star, fold axis of crenulation event (L_3). d, Poles to crenulation cleavage from Dead Man Canyon area. +, fold axes (L_3); filled triangles, poles to axial planes of mesoscopic folds (S_3); open triangles, poles to crenulation cleavages (S_3).

bedding-parallel folds. Evidence for this generation of folds is not seen in the more competent quartzite and granitic units. The second phase (D_2) is associated with open to tight, upright folds with rounded hinges and limbs. A penetrative axial planar cleavage is subvertical and strikes northwest to west-northwest. The final phase of folding (F_3) is a low-strain event that reoriented the S_2 cleavage into open kink folds. A pluton that contains the S_2 and S_3 foliations has been dated at 1632 ± 24 Ma, providing a maximum age for D_2.

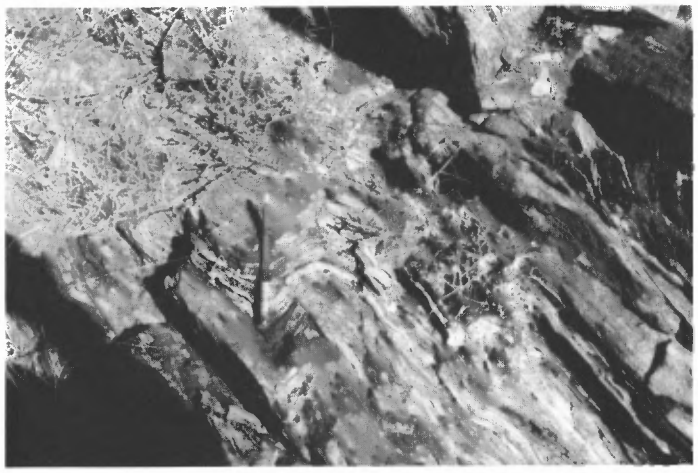

FIGURE 5. Mesoscopic fold in metasedimentary units south of Dead Man Canyon. Axial plane strikes N50°W. Pencil is 13 cm long.

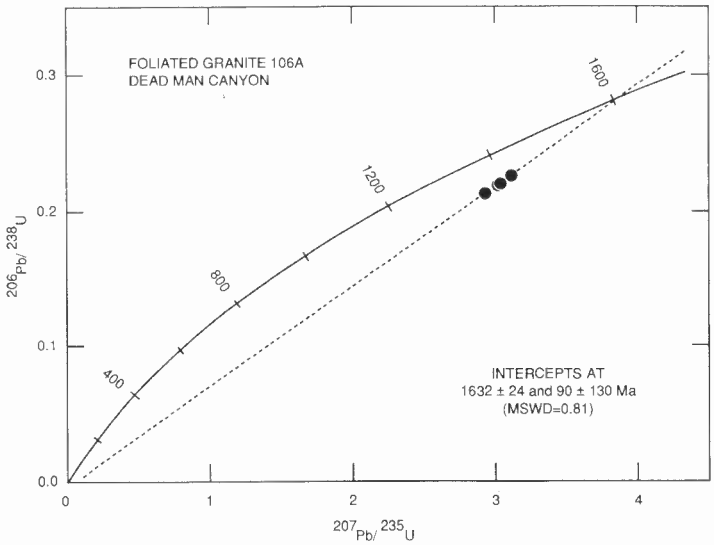

FIGURE 6. U-Pb concordia diagram showing age of foliated granite (Sample #106A) from Dead Man Canyon. Location of sample shown on Fig. 2.

Ages similar to that of the foliated pluton, 1632 ± 24 Ma, have been reported from other areas in central and southern New Mexico. Bowring et al. (1983) reported an age of 1650 ± 10 Ma (U-Pb zircon) for metamorphosed volcanic rocks and associated plutons in the Socorro area (Fig. 1). A granophyre from the southern Black Range is approximately 1655 Ma old (U-Pb zircon) (Stacey and Hedlund, 1983).

LITTLE SAN NICOLAS CANYON

An 18 km^2 (7 mi^2) area was mapped in Little San Nicolas Canyon (Fig. 7). The three rocks recognized are granitic plutons, amphibolite and banded gneiss. Float of a foliated granite similar to that found in Dead Man Canyon is common in the canyon alluvium, but outcrop was not found in the map area. The gneiss is exposed along a series of high-angle reverse faults. It is composed of well-defined dark and light bands, ranging in thickness from a millimeter in some localities to a centimeter in others. No lithologic differences are apparent in outcrop. The dark

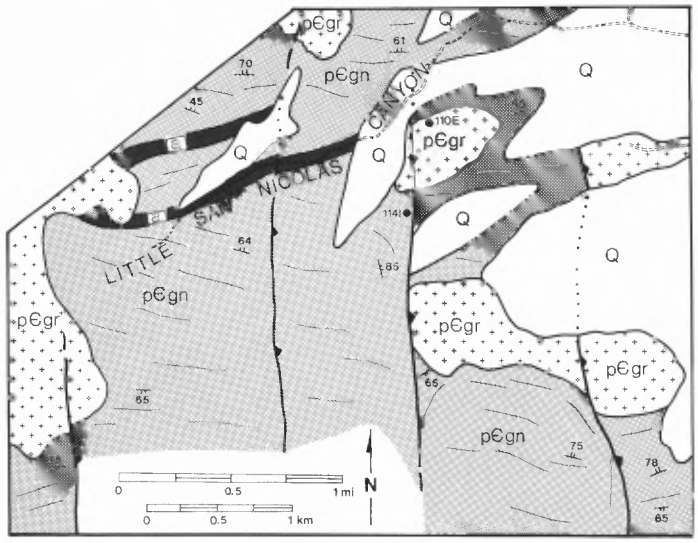

FIGURE 7. Generalized geologic map of Little San Nicolas Canyon. pЄgn, gneiss; pЄgr, undeformed granite; a, Precambrian amphibolite; Q, Quaternary alluvium. Thick lines mark reverse faults, with teeth on hanging wall. Fine lines mark trend of gneissic foliation. Strike and dip symbols show attitude of gneissic foliation. Filled circles mark sample locations for U-Pb dating. See Fig. 1 for location of Little San Nicolas Canyon.

bands are composed primarily of biotite, the light bands of quartz and feldspar. Large anhedral, poikiloblastic garnets crosscut the layering.

The amphibolites in the study area are similar in composition to those in Dead Man Canyon. They are composed primarily of amphibole and plagioclase with subordinate quartz. These mafic bodies are unfoliated and are oriented subparallel to the general trend of the gneissic foliation (Fig. 8).

The largest pluton in Little San Nicolas Canyon is a quartz monzonite known as the Mineral Hill granite (Condie and Budding, 1979). A smaller white, garnet-bearing pluton is also present in the western end of the study area. It is composed of equal proportions of plagioclase, potassium feldspar and quartz, making it a true granite, with minor amounts of biotite and opaque minerals. Red, subhedral garnets are prominent in hand sample.

Structural analysis

The gneiss in Little San Nicolas Canyon shows evidence of two phases of deformation. The earlier generation is defined by a gneissic foliation (S_1), which is composed of bands of dark and light minerals (Fig. 8). S_1 was then refolded into upright, tight to isoclinal, west-plunging folds (Fig. 9). The axial plane of the F_2 folds is steeply dipping, and strikes approximately east-west. No axial planar cleavage was observed.

Several large north-striking reverse faults crosscut these units. They dip steeply to the east, and are marked by lines of springs and 2-to-5-m-thick zones of fault breccia (Fig. 10). Faults similar to these were described by Seager (1981) farther south in the San Andres and Organ Mountains. Using field relationships, he interpreted these structures to be of Laramide age (40–60 Ma). This correlates with the age of lead loss in the zircons from Little San Nicolas Canyon. However, there is evidence that these faults may have a more complex history. S. Kelley (pers. comm., 1991) obtained fission-track ages on apatites extracted from both the gneiss (Sample #114I) and on a sample of the garnet-bearing granite. Uplift ages were 8 Ma for the gneiss and 21 Ma for the garnet-bearing granite, significantly younger than Laramide. These Laramide faults may have been reactivated as normal faults in the late Tertiary.

Geochronology

Zircons obtained from the gneiss (Sample #114I; Fig. 7) give an age of 1730 ± 130 Ma (MSWD = 8.6; Fig. 11). Although these zircons are clear, euhedral and inclusion-free, they are metamict and highly discordant. The data points cluster in the middle of the chord, making the errors at both intercepts equally large. A separate sample of the gneiss was processed for whole-rock Sm-Nd dating. This sample yielded a model age of 1.81 Ga, corroborating the U-Pb zircon age.

A coarse-grained, gray granite was collected from Little San Nicolas Canyon (Fig. 8). Zircons from this sample (Sample #110E) give an age of 1462 ± 67 Ma (MSWD = 12.2; Fig. 12). White (1977) reported a Rb-Sr whole-rock age of 1190 ± 161 Ma and an initial strontium ratio of .7118 for the Mineral Hill pluton (recalculated using the decay constants of Steiger and Jager, 1977). The sample of garnet-bearing granite lacked sufficient zircon for dating.

FIGURE 8. Folded gneiss in Little San Nicolas Canyon. South is to the top. Pen is 13 cm long. Folds plunge gently to the west.

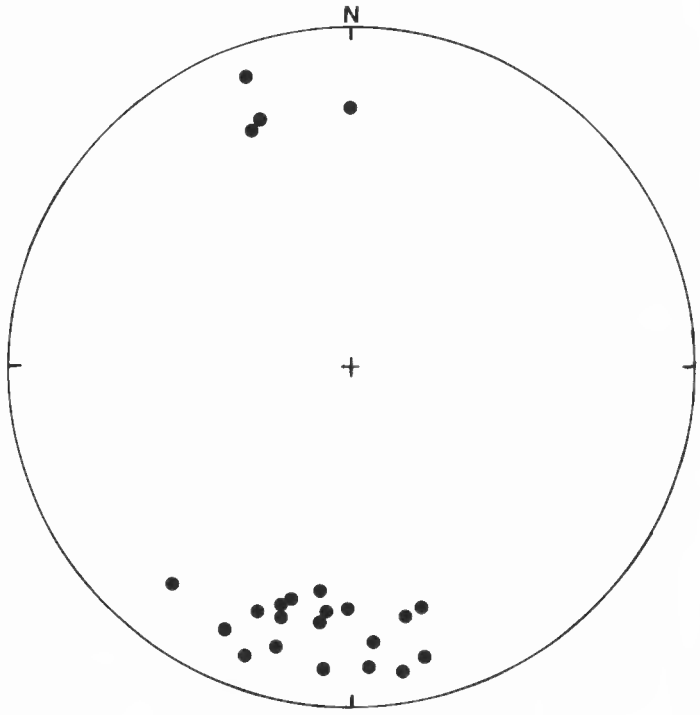

FIGURE 9. Lower hemisphere, equal area stereonet of gneissic foliation data from Little San Nicolas Canyon.

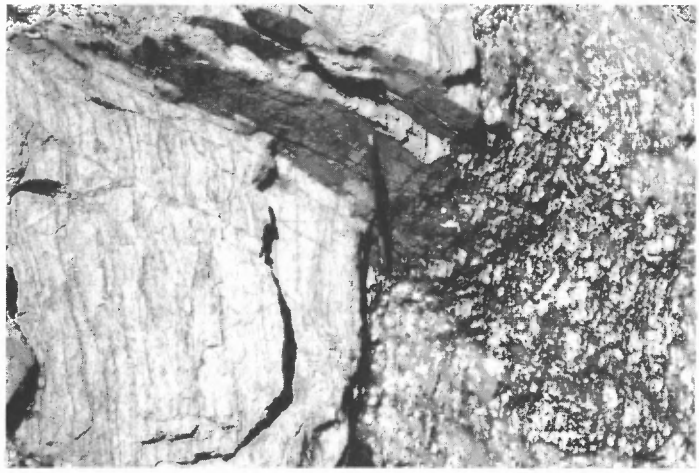

FIGURE 10. High-angle fault in granite striking N5°W and plunging 85° to the east. Photo is cross-section view, looking south.

Summary and discussion

The predominant rock type in Little San Nicolas Canyon is a homogeneous, well-banded gneiss. This gneiss displays evidence for two periods of folding, the early phase generating the mineral banding and the second refolding it. The study area is cut by several large, east-dipping thrust faults. Similar faults were interpreted as Laramide by Seager (1980). However, evidence from fission-track ages suggests that these faults may have been reactivated during the late Tertiary as normal faults (S. Kelley, pers. comm., 1991). Zircons extracted from the gneiss

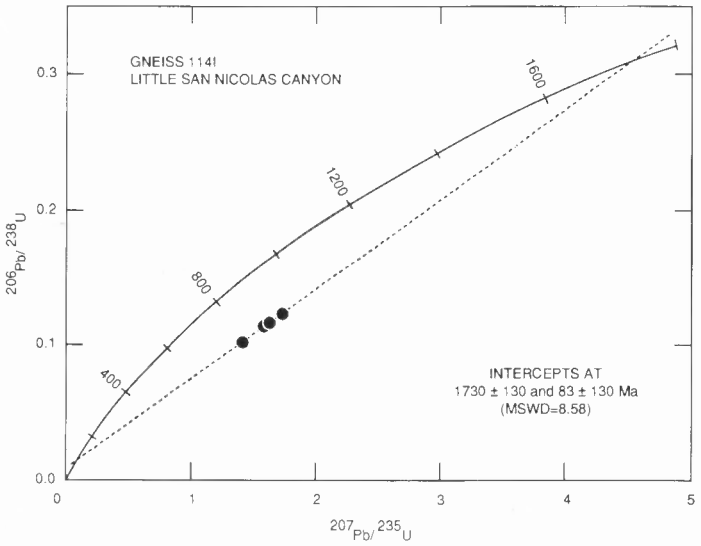

FIGURE 11. U-Pb concordia diagram showing age of gneiss (Sample 114I) from Little San Nicolas Canyon. Location of sample shown on Fig. 7.

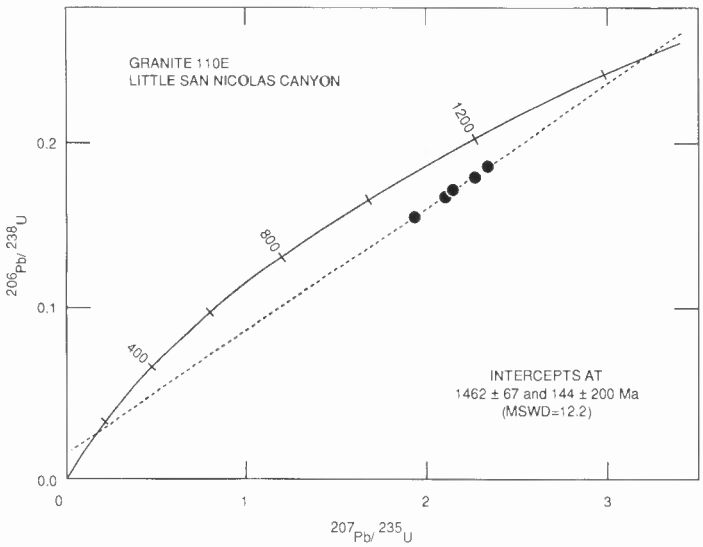

FIGURE 12. U-Pb concordia diagram showing age of post-orogenic granite (Sample 110E) from Little San Nicolas Canyon. Location of sample shown on Fig. 7.

are highly discordant, but yield an age of 1730 ± 130 Ma. This age is corroborated by one Sm-Nd whole rock model age of 1.81 Ga. One unfoliated granite has a U-Pb zircon age of 1462 ± 67 Ma.

The protolith of the gneiss exposed in Little San Nicolas Canyon is unknown. This gneiss is quartzo-feldspathic and, except for garnet, lacks metamorphic minerals that could be expected in metamorphosed pelitic units. Also, the zircons extracted from the gneiss are clear and euhedral, suggesting that they are of igneous origin. It seems most likely that this gneiss formed from felsic igneous rocks, possibly plutonic.

SUMMARY

In Dead Man Canyon, a series of metasedimentary rocks is overlain by a micaceous quartzite. Three generations of folding have been identified. An early, bedding-parallel, isoclinal phase affected only the schists in the metasedimentary units. The second deformation formed the northwest-trending slaty cleavage (S_2) that is the dominant structural fabric throughout the study area. Evidence of this second event is found not only in the metasedimentary rocks, but in a pluton that intrudes them. This foliated granite has been dated at 1632 ± 24 Ma. The final event, D_3, is a crenulation event that refolded the S_2 cleavage into reclined, open kink folds. The crenulation cleavage, S_3, is weakly developed throughout the study area. The youngest Precambrian unit in the Dead Man Canyon area is the unfoliated Mayberry pluton, dated by White (1977) at 1248 ± 170 Ma.

In the southern area, Little San Nicolas Canyon, the outcrop is predominantly composed of gneiss and undeformed granite. Two deformational events were identified in the gneiss. The first resulted in well-developed metamorphic banding. The second event refolded the metamorphic foliation around a west-plunging axis. Highly discordant zircons extracted from the gneiss give an age of 1730 ± 130 Ma; zircons extracted from an unfoliated pluton yield a date of 1462 ± 67 Ma.

The relationship between the gneiss in the southern area and the metasediments in the northern area is unknown. Although the canyons are only 32 km apart, the rocks exposed in each area are quite different. In the Dead Man Canyon area, sedimentary structures are generally well preserved, and lithological differences are easily observed. In Little San Nicolas Canyon, the gneiss is essentially homogeneous and any original textures that may have been present have been obliterated by metamorphism.

ACKNOWLEDGMENTS

I thank the U.S. Army for granting permission to enter White Sands Missile Range, and Sam Seek and Rod Pena for easing the process. Thanks also go to P. Bauer, R. Lozinsky and J. Robertson for reviewing this manuscript and suggesting many improvements.

REFERENCES

Bauer, P. W. and Lozinsky, R. P., 1986, Proterozoic geology of supracrustal and granitic rocks in the Caballo Mountains, southern New Mexico: New Mexico Geological Society, Guidebook 37, p. 143–149.

Bowring, S. A., Kent, S. C. and Sumner, W., 1983, Geology and U-Pb geochronology of Proterozoic rocks in the vicinity of Socorro, New Mexico: New Mexico Geological Society, Guidebook 34, p. 137–142.

Condie, K. C. and Budding, A. J., 1979, Geology and geochemistry of Precambrian rocks, central and south-central New Mexico: New Mexico Bureau of Mines and Mineral Resources, Memoir 35, 58 p.

Ludwig, K. R., 1980, Calculation of uncertainties of U-Pb isotope data: Earth and Planetary Science Letters, v. 46, p. 212–220.

Parrish, R. R., 1987, An improved micro-capsule for zircon dissolution in U-Pb geochronology: Chemical Geology (Isotope Geoscience Section), v. 66, p. 99–102.

Roths, P., 1991, Preliminary results of investigation of Proterozoic outcrops, southern San Andres Mountains, N.M.: Geological Society of America, Abstracts with Programs, v. 23, p. 88.

Seager, W. R., 1981, Geology of Organ Mountains and southern San Andres Mountains, New Mexico: New Mexico Bureau of Mines and Mineral Resources, Memoir 36, 97 p.

Stacey, J. S. and Hedlund, D. C., 1983, Lead-isotopic compositions of diverse igneous rocks and ore deposits from southwestern New Mexico and their implications for early Proterozoic crustal evolution in the western United States: Geological Society of America Bulletin, v. 94, p. 43–57.

White, D. L., 1977, A Rb-Sr study of the Precambrian intrusives of south-central New Mexico [Ph.D. dissertation]: Oxford, Ohio, Miami University, 88 p.

APPENDIX

For U-Pb zircon geochronology, 40 to 60 lbs of sample were crushed, sieved, and nonmagnetic zircons were separated. These were cleaned by boiling in HNO_3 and HCl before dissolution in modified Parrish bombs (Parrish, 1987). Total processing blanks were 20 to 40 picograms of lead. Analyses were carried out on a Finnegan MAT 261 mass spectrometer at the University of Texas at Dallas (Table 1). Regression calculations to concordia are those of Ludwig (1980); uncertainties are at the 95% confidence level.

TABLE 1. U and Pb concentration and isotopic composition data.

Sample, mesh	Concentration U, ppm	Pb, ppm	Measured Pb ratios 206/204	207/206	Corrected ratios 207Pb/235U	206Pb/238U
106 A, foliated granite[1].						
140-170	301.4	70.36	5555	0.10219	3.0393	0.22120
200-230	307.1	71.54	2381	0.10534	3.0208	0.22019
230-270	289.1	69.60	3571	0.10367	3.1205	0.22686
<325	320.2	72.71	6250	0.10198	2.9402	0.21414
114 I, gneiss[2].						
140-170	618.4	65.77	3846	0.10441	1.4159	0.10189
170-200	632.8	74.01	4167	0.10441	1.5856	0.11380
200-230	656.8	78.51	3846	0.10492	1.6172	0.11579
<270	612.6	77.72	4167	0.10551	1.7331	0.12304
110 E, granite[3].						
100-140	317.4	66.08	1724	0.09863	2.2639	0.18143
140-170	494.8	106.89	3333	0.09425	2.3289	0.18764
170-200	490.7	88.91	4348	0.09236	1.9282	0.15696
200-230	278.8	55.34	3846	0.09358	2.1015	0.16952
<270	419.8	85.24	2326	0.0955	2.1431	0.17376

1. Common lead correction at 1600 Ma (Stacey and Kramers, 1975)
2. Common lead correction at 1750 Ma (Stacey and Kramers, 1975)
3. Common lead correction at 1500 Ma (Stacey and Kramers, 1975)